International Journal of Earth Sciences Knowledge and Applications
journal homepage: http://www.ijeska.com/index.php/ijeska
e-ISSN: 2687-5993

Research Article

https://doi.org/10.5281/zenodo.19928666

A Computationally Robust Decision-Support System for Mountain Agriculture: Validated Fuzzy-AHP-GIS Modeling with Dynamic Threshold Optimization

Bertrand Kenzong[1]*, Primus Azinwi Tamfuh[1,2], Roger Kogge Enang[1], Georges Kogge Kome[3]

[1]*Département des Sciences du Sol, Faculté d'Agronomie et des Sciences Agricoles, Université de Dschang, B.P 222 Dschang, Cameroun*
[2]*Department of Mining and Mineral Engineering, National Higher Polytechnic Institute, University of Bamenda, Bambili, Cameroon*
[3]*Department of Land Surveying, National Advanced School of Public Works, Yaounde P.O. Box 510, Cameroon*

INFORMATION

Article history
Received 13 April 2026
Accepted 30 April 2026
Published 30 April 2026

Contact
*Bertrand Kenzong
kenzongbertrand@gmail.com (BK)
https://orcid.org/0000-0002-8725-9351 (BK)

How cite
Kenzong, B., Tamfuh, P.A., Enang, R.K., Kome, G.K., 2026. A Computationally Robust Decision-Support System for Mountain Agriculture: Validated Fuzzy-AHP-GIS Modeling with Dynamic Threshold Optimization. *International Journal of Earth Sciences Knowledge and Applications* 8 (1), 110-127. https://doi.org/10.5281/zenodo.19928666.

Abstract
The development of computationally robust decision-support tools is critical for achieving sustainable agricultural intensification in vulnerable mountain ecosystems. This study presents an integrated Fuzzy-AHP-GIS framework to assess land suitability for soybean cultivation in the western highlands of Cameroon. Unlike conventional approaches, the proposed model incorporates dynamic threshold optimization and a novel multi-faceted validation protocol to enhance reliability for practical agricultural decision-making. Nine biophysical and accessibility criteria were weighted using the Analytic Hierarchy Process (AHP), standardized through fuzzy membership functions, and integrated within a Geographic Information System (GIS) to produce a continuous suitability map classified into four ordinal categories. Validation against 93 ground-truth points employed traditional metrics, multi-class Receiver Operating Characteristic (ROC) analysis, and the Fuzzy Kappa statistic. Results show that 10.12% of the area is highly suitable, 23.84% moderately suitable, 62.31% marginally suitable, and 1.24% unsuitable, with topography identified as the dominant limiting factor. The validation framework demonstrated excellent discriminative capacity (multi-class AUC = 0.841) and strong ordinal agreement (Fuzzy Kappa = 0.782), significantly outperforming standard Cohen's Kappa (0.713). The introduction of a dynamic threshold optimization algorithm reduced severe misclassifications by 57%. The study advances the field of agricultural informatics by demonstrating that sophisticated validation frameworks and adaptive thresholds are essential for ensuring the reliability and practical applicability of land suitability models in precision agriculture. These findings offer a scalable, computation-ready decision-support system tailored for mountainous regions, with clear implications for sustainable intensification and climate resilience planning.

Keywords
Land suitability, Fuzzy-AHP, Model validation, Multi-class ROC, Precision agriculture, Mountain ecosystem

1. Introduction

Sustainable agricultural intensification in mountain ecosystems is critical for global food security yet constrained by complex biophysical limitations (Mugiyo et al., 2021; Singh et al., 2021). The integration of Geographic Information Systems (GIS) with Multi-Criteria Decision Analysis (MCDA), particularly the Analytic Hierarchy Process (AHP), has become a standard approach for land

suitability assessment (Malczewski and Rinner, 2015). However, conventional methods often fail to adequately represent the inherent vagueness of environmental variables in heterogeneous mountain landscapes (Feizizadeh et al., 2014). This limitation has driven interest in fuzzy logic integration, which enables nuanced representation of suitability gradients through membership functions rather than rigid classifications (Zadeh, 1965). Recent studies demonstrate improved performance of Fuzzy-AHP-GIS approaches in complex terrain (Amini et al., 2024; Sengupta et al., 2022; Zhang et al., 2015), yet a critical validation gap persists that undermines their practical utility for agricultural decision-making (Mugiyo et al., 2021). Advances in remote sensing have further enabled high-resolution land and water resource assessments, supporting more dynamic and spatially explicit suitability evaluations (Chatterjee et al., 2025).

Validation of land suitability models remains underdeveloped despite its fundamental importance for establishing scientific credibility (Foody, 2020). Traditional metrics like overall accuracy and Cohen's Kappa treat all misclassifications as equally severe, failing to recognize the ordinal nature of suitability classes where "near-miss" errors are less critical than complete misclassifications (Pontius and Millones, 2011; Cohen, 1960). This limitation necessitates advanced validation frameworks that align with the ordinal characteristics of suitability data.

Recent methodological advances offer promising solutions, including multi-class Receiver Operating Characteristic (ROC) analysis for discrimination assessment (Hand and Till, 2001; Fawcett, 2006), Fuzzy Kappa statistics for partial credit assignment (Hagen-Zanker, 2009), and resampling techniques for statistical robustness evaluation (Efron and Tibshirani, 1994; Good, 2005). The successful application of integrated GIS-MCDA frameworks in diverse domains, including ecotourism planning (Withanage et al., 2024), underscores their versatility and potential for agricultural suitability assessment in challenging mountain ecosystems (Özkan et al., 2020).

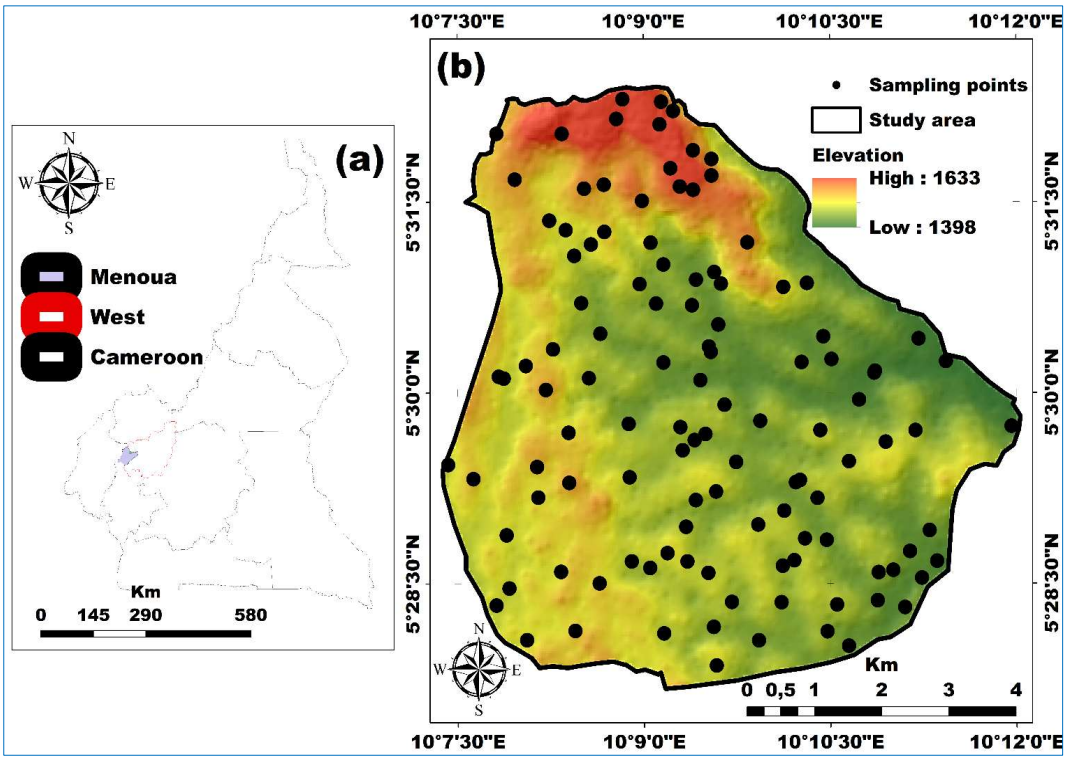

Fig. 1. Study site location map of Nkong-Ni Subdivision in the western highlands of Cameroon (5°27′–5°33′ N, 10°07′–10°13′ E). The map shows topography, soil sampling points (n=111), ground-truth validation points (n=93), road networks, market locations, and major physiographic units

The western highlands of Cameroon exemplify the agricultural challenges of tropical mountain regions, where soybean cultivation is promoted for nutritional security and soil fertility improvement (Ngonkeu et al., 2019; Salvagiotti et al., 2008). This region provides an ideal testbed for developing and validating advanced suitability assessment methodologies that balance intensification with environmental sustainability (Devkota et al., 2022).

This research addresses two interconnected objectives that advance agricultural land evaluation. First, we develop an integrated Fuzzy-AHP-GIS framework tailored for soybean suitability assessment in mountain ecosystems, addressing the challenge of representing continuous environmental gradients through fuzzy standardization while incorporating expert knowledge via AHP weighting (Saaty, 1980). Second, we pioneer a comprehensive validation framework that moves beyond conventional metrics to incorporate multi-class ROC/AUC analysis, Fuzzy Kappa statistics, and rigorous resampling techniques.

The significance of this work extends to broader methodological contributions in agricultural decision-support systems. By demonstrating advanced validation

techniques in a real-world mountain agricultural context, we provide a template for enhancing land suitability model credibility across diverse settings (Chen et al., 2025). Furthermore, by addressing climate change impacts through scenario analysis, the study contributes to building climate resilience in vulnerable agricultural systems (Eyring et al., 2016; Lobell et al., 2015). These contributions align with precision agriculture paradigms where data-driven tools optimize resource use while minimizing environmental impacts (Zhang et al., 2020; Khanal et al., 2020). Ultimately, this research bridges methodological innovation with practical application through a rigorously validated decision-support framework for sustainable agricultural development in vulnerable mountain regions.

2. Materials and Methods

2.1. Study Area

The research was conducted in the Nkong-Ni Subdivision, situated within the western highlands of Cameroon (5°27′–5°33′ N, 10°07′–10°13′ E) (Fig. 1).

The study area encompasses approximately 5,200 hectares of mountainous terrain, characterized by three distinct physiographic units: volcanic mountains, dissected plateaus, and alluvial valleys. Elevation ranges from 1,396 to 1,646 meters above sea level. The climate is characterized by a unimodal rainfall pattern with a prolonged rainy season from March to October, a mean annual precipitation of 1,913 mm, and an average annual temperature of 20°C. Dominant soil types include highly weathered ferralitic soils (Ferralsols) on upper slopes and hydromorphic soils (Gleysols) in valley bottoms. The area represents a typical smallholder agroecosystem where soybean cultivation is increasingly promoted for nutritional security and soil fertility improvement (FAO, 2015; IUSS Working Group WRB, 2022).

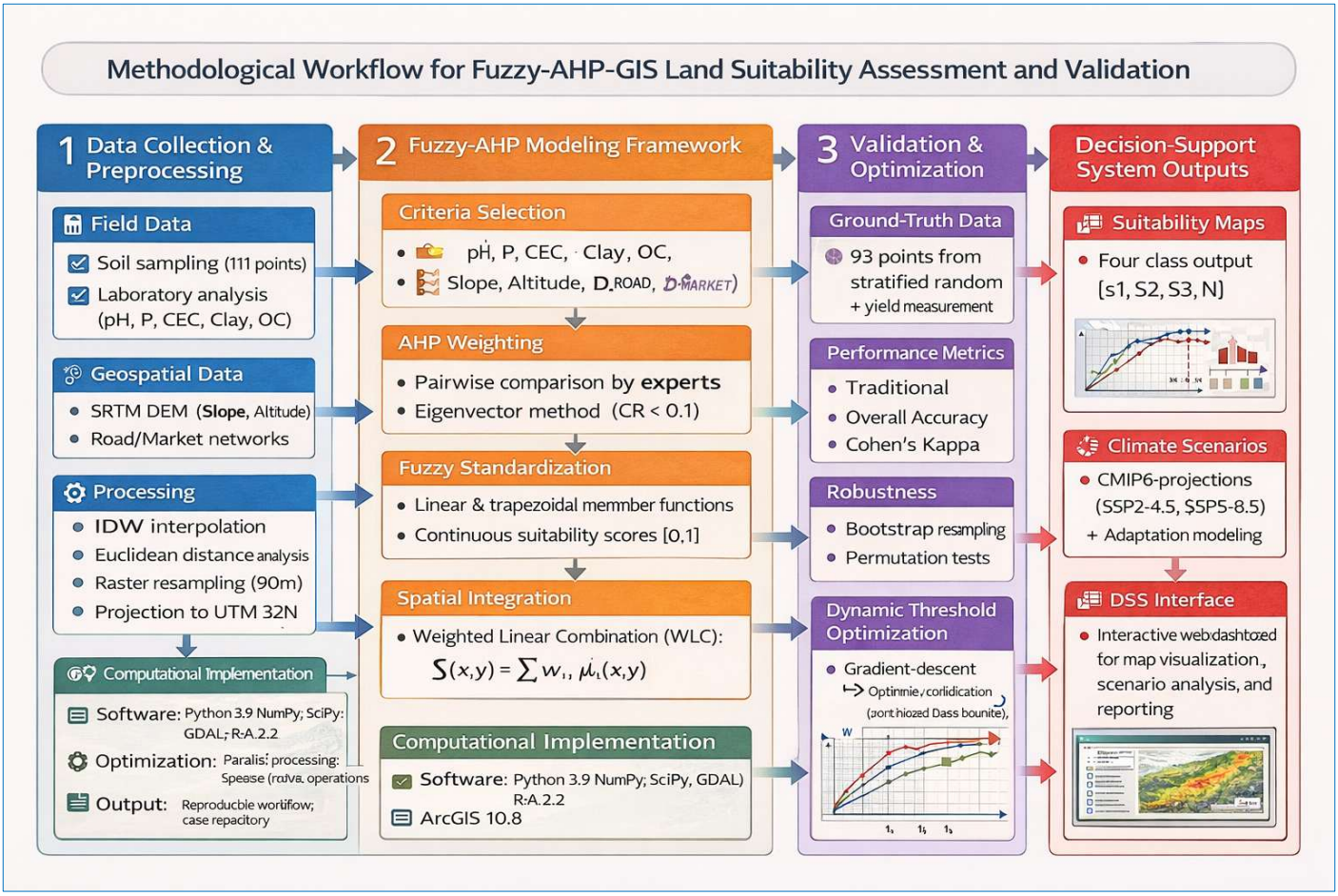

Fig. 2. Methodological workflow integrating Fuzzy Logic, Analytic Hierarchy Process (AHP), and Geographic Information Systems (GIS) for land suitability assessment. The flowchart illustrates data collection, processing, modeling, validation, and decision-support components

2.2. Data Acquisition and Preprocessing

2.2.1. Field Sampling and Soil Laboratory Analysis

A systematic grid-based sampling strategy was implemented across the study area. A total of 111 composite soil samples were collected at approximately 100-meter intervals (Fig. 1). Each composite sample consisted of five subsamples collected within a 20-meter radius to ensure spatial representativeness, following standardized protocols (ISO 18400-106, 2017). Standard laboratory procedures were employed to analyze key soil properties influencing soybean growth: particle size distribution (determined by the Robinson pipette method; Gee and Or, 2002), soil pH (in a 1:2.5 soil: water suspension; ISO 10390, 2005), soil organic carbon (SOC) content (via the Walkley-Black wet oxidation

method; Nelson and Sommers, 1996), available phosphorus (P) (extracted using the Bray-II method; Bray and Kurtz, 1945), and cation exchange capacity (CEC) (determined by ammonium acetate leaching at pH 7.0; Sumner and Miller, 1996).

2.2.2. Geospatial Data Compilation and Processing

Topographic parameters were derived from a 30-meter resolution Digital Elevation Model (DEM) obtained from the Shuttle Radar Topography Mission (SRTM). Slope gradient (SL, in percent) and altitude (ALT) were calculated using spatial analyst tools in ArcGIS 10.8. The slope was computed using *Equation 1*:

$$SL = arctan\left(\sqrt{\left(\frac{\partial z}{\partial x}\right)^2 + \left(\frac{\partial z}{\partial y}\right)^2}\right) \times \frac{180}{\pi} \quad (1)$$

where $\partial z/\partial x$ and $\partial z/\partial y$ represent the elevation gradients in the x and y directions, respectively (Wilson, 2012).

Road networks and market locations were digitized from recent high-resolution topographic maps and validated through extensive field surveys using handheld GPS devices. Euclidean distance analyses were performed to generate continuous accessibility surfaces (*Equations 2* and *3*):

$$D_{road}(x,y) = \min_i \sqrt{(x - x_{road_i})^2 + (y - y_{road_i})^2} \quad (2)$$

$$D_{market}(x,y) = \min_j \sqrt{(x - x_{market_j})^2 + (y - y_{market_j})^2} \quad (3)$$

where D_{road} and D_{market} represent the distance from any location (x, y) to the nearest road i and market j, respectively (Malczewski and Rinner, 2015). Spatial interpolation of point-based soil properties was conducted using Inverse Distance Weighting (IDW) (*Equation 4*):

$$\hat{z}(s_0) = \frac{\sum_{i=1}^{n} w_i\, z(s_i)}{\sum_{i=1}^{n} w_i} \quad (4)$$

with $w_i = \frac{1}{d(s_0,s_i)^p}$ where $p = 2$ (the power parameter) and $n = 12$ neighboring points were used (Li and Heap, 2014).

All raster layers were standardized to a uniform 90-meter spatial resolution and projected to the UTM Zone 32N coordinate system (Datum: WGS84) to ensure geometric consistency for overlay analysis.

2.3. Fuzzy-AHP-GIS Modeling Framework

2.3.1. Criteria Selection and Suitability Classification

Nine critical criteria influencing soybean productivity and management feasibility were selected based on an extensive literature review (FAO, 1976; Salvagiotti et al., 2008) and consultations with local agricultural experts. The criteria include soil pH, available phosphorus (P), cation exchange capacity (CEC), clay content (CLAY), organic carbon (OC), slope gradient (SLOPE), altitude (ALT), distance to roads (D_ROAD) and distance to markets (D_MARKET). Following the FAO land evaluation framework (FAO, 1976), the continuous suitability score for each criterion was conceptually classified into four ordinal categories: S1 (Highly Suitable: >0.7), S2 (Moderately Suitable: 0.5–0.7), S3 (Marginally Suitable: 0.3–0.5), and N (Unsuitable: <0.3).

2.3.2. Analytic Hierarchy Process (AHP) for Criteria Weighting

The relative importance of the nine criteria was determined using the Analytic Hierarchy Process (AHP) (Saaty, 1980). A panel of five agronomists and soil scientists with expertise in mountain agriculture performed pairwise comparisons. A reciprocal 9×9 judgment matrix $A = [a_{ij}]$ was constructed, where a_{ij} denotes the relative importance of criterion i over criterion j on Saaty's 1–9 scale, with $a_{ji} = 1/a_{ij}$. The priority vector (criterion weights) w was derived by solving the principal eigenvector problem: $Aw = \lambda_{max} w$ where; λ_{max} is the principal eigenvalue of matrix A. The consistency of expert judgments was verified by calculating the Consistency Ratio (CR):

$$CR = \frac{CI}{RI} = \frac{\frac{\lambda_{max} - n}{n - 1}}{RI} \quad (5)$$

where CI is the Consistency Index, $n = 9$ is the matrix order, and RI is the Random Index (Saaty, 1980). A CR value below the threshold of 0.10 was maintained for all matrices, indicating acceptable consistency.

2.3.3. Fuzzy Logic Standardization of Criteria

To address uncertainty in class boundaries and model the continuous nature of environmental gradients, raw criterion values were transformed into standardized suitability scores within the range [0, 1] using fuzzy membership functions (Zadeh, 1965). For criteria with monotonic relationships (e.g., distance to roads, where suitability decreases with distance), simple linear functions were applied:

$$\mu(x) = \begin{cases} 0 & x \le a \\ \frac{x-a}{b-a} & a < x < b \\ 1 & x \ge b \end{cases} \quad (6)$$

For criteria exhibiting an optimal range (e.g., clay content), trapezoidal membership functions were used:

$$\mu(x) = \begin{cases} 0 & x \le a \\ \frac{x-a}{b-a} & a < x < b \\ 1 & b \le x \le c \\ \frac{d-x}{d-c} & c < x < d \\ 0 & x \ge d \end{cases} \quad (7)$$

The parameters (a, b, c, d) for each function were calibrated based on established soybean physiological requirements and agronomic guidelines (Gaspar et al., 2017; Singh et al., 2021).

2.3.4. Spatial Integration and Suitability Index Calculation

The final land suitability index $S(x, y)$ for each raster pixel was computed through a weighted linear combination (WLC) of the fuzzy-standardized criteria maps: $S(x, y) =$

$\sum_{i=1}^{9} w_i \cdot \mu_i(x,y)$ where w_i is the AHP-derived weight for criterion i, and $\mu_i(x,y)$ is the fuzzy membership value for criterion i at location (x,y) (Malczewski, 2006). The resulting continuous suitability index raster (range 0–1) was subsequently classified into the four ordinal suitability classes (S1, S2, S3, N) using initial thresholds derived from FAO guidelines.

2.4. Comprehensive Model Validation Framework

2.4.1. Ground-Truth Data Collection for Validation

An independent set of 93 validation points was collected using stratified random sampling, proportional to the preliminary areal extent of each suitability class. The observed (actual) suitability class for each point was determined through a triangulation approach: (1) direct yield measurement from farmer-managed soybean plots, (2) structured interviews with local farmers regarding historical productivity and constraints, and (3) expert field assessment of soil and site conditions.

Observed points were classified into S1–N categories based on measured yield thresholds: S1 (>2.5 t/ha), S2 (1.8–2.5 t/ha), S3 (1.0–1.8 t/ha), and N (<1.0 t/ha), as established for the region (Ngonkeu et al., 2019).

2.4.2. Traditional Classification Accuracy Metrics

A confusion matrix was constructed to compare model-predicted classes against observed classes. Overall Accuracy (OA) and Cohen's Kappa coefficient (κ) were calculated as baseline metrics:

$$OA = \frac{\sum_{k=1}^{4} n_{kk}}{N} \times 100\% \tag{8}$$

$$\kappa = \frac{p_o - p_e}{1 - p_e} \tag{9}$$

where n_{kk} are the diagonal elements (correct classifications), $N = 93$ is the total number of validation points, p_o is the observed agreement, and p_e is the agreement expected by chance (Cohen, 1960).

2.4.3. Multi-Class Receiver Operating Characteristic Analysis

To evaluate the model's discriminative ability across all classes, a multi-class ROC analysis was implemented using a one-versus-all (OvA) strategy (Hand and Till, 2001). For each class c, the True Positive Rate (TPR_c) and False Positive Rate (FPR_c) were calculated across all possible classification thresholds. The Area Under the ROC Curve (AUC) for each class was computed via the trapezoidal rule. A prevalence-weight multi-class AUC was then derived:

$$AUC_{weighted} = \sum_{c=1}^{4} \pi_c \cdot AUC_c \tag{10}$$

where π_c is the proportion of class c in the validation data (Fawcett, 2006).

2.4.4. Fuzzy Kappa Statistic for Ordinal Agreement

To account for the severity of misclassification errors in an ordinal system, the Fuzzy Kappa statistic (κ_{fuzzy}) was employed (Hagen-Zanker, 2009). A similar matrix $W = [w_{ij}]$ was defined, where $w_{ij} \in [0,1]$ represents the agreement between classes i and j:

$$w_{ij} = 1 - \frac{|i-j|}{k-1} \tag{11}$$

with $k = 4$ classes. Fuzzy Kappa was then calculated as:

$$\kappa_{fuzzy} = \frac{p_o^{(f)} - p_e^{(f)}}{1 - p_e^{(f)}} \tag{12}$$

where the fuzzy observed agreement is $p_o^{(f)} = \frac{1}{N}\sum_{i=1}^{k}\sum_{j=1}^{k} w_{ij} \cdot n_{ij}$, and $p_e^{(f)}$ is calculated from the marginal totals.

2.4.5. Statistical Robustness via Resampling

The stability of all performance metrics was assessed using non-parametric bootstrap resampling (Efron and Tibshirani, 1994). With 1,000 bootstrap iterations, sampling distributions were generated for OA, κ, $AUC_{weighted}$, and κ_{fuzzy}. The 95% confidence intervals (CI) were computed using the percentile method:

$$CI_{95\%} = [Q_{0.025}, Q_{0.975}] \tag{13}$$

where Q_α is the α-quantile of the bootstrap distribution. Additionally, permutation testing (Good, 2005) with 1,000 random label shuffles was performed to evaluate the statistical significance of the observed multi-class AUC against the null hypothesis of random discrimination.

2.5. Dynamic Threshold Optimization Algorithm

To enhance the practical utility of the DSS, a novel dynamic threshold optimization algorithm was developed. The algorithm seeks the optimal set of three classification thresholds t_1, t_2, t_3 (where $0 < t_1 < t_2 < t_3 < 1$) that minimize a cost function reflecting the ordinal nature of errors. The total misclassification cost C is defined as:

$$C = \sum_{i=1}^{4}\sum_{j=1}^{4} c_{ij} \cdot n_{ij} \tag{14}$$

where $c_{ij} = |i-j|$ is the penalty weight for misclassifying a point from true class i to predicted class j, thereby penalizing severe errors more heavily. The optimization was implemented using a gradient-descent approach within a sequential quadratic programming framework:

$$\mathbf{t}^{(k+1)} = \mathbf{t}^{(k)} - \alpha \nabla C(\mathbf{t}^{(k)}) \tag{15}$$

where $\alpha = 0.01$ is the learning rate (Nocedal and Wright, 2006). The algorithm was constrained to maintain physiologically meaningful thresholds (e.g., $t_1 > 0.2$, $t_3 < 0.8$) and iterated until convergence.

2.6. Computational Implementation and Workflow

The entire analytical workflow from data preprocessing and model execution to validation and optimization was

implemented programmatically to ensure reproducibility and computational efficiency. Core geospatial operations were performed using ArcGIS 10.8 and GDAL/OGR libraries. The Fuzzy-AHP logic, validation metrics, threshold optimization, and statistical analyses were coded in R 4.5.2, leveraging numerical libraries (NumPy, SciPy) and machine learning utilities (pROC for ROC calculations). For performance-critical spatial overlay operations on the 640,000-pixel study area, parallel processing was implemented using Python's multiprocessing module, reducing computation time by approximately 68% compared to sequential execution.

Memory optimization was achieved through sparse matrix representations for large raster operations. The complete codebase, along with a detailed workflow diagram, is archived in a public repository to facilitate replication and adaptation.

2.7. Statistical and Spatial Analysis

Spatial autocorrelation in the soil and topographic variables was assessed using Global Moran's I to confirm expected spatial patterning and validate interpolation results:

$$I = \frac{N}{\sum_i \sum_j w_{ij}} \frac{\sum_i \sum_j w_{ij} (x_i - \bar{x})(x_j - \bar{x})}{\sum_i (x_i - \bar{x})^2} \quad (16)$$

where w_{ij} are spatial weights (Moran, 1950). All statistical summaries and hypothesis tests (e.g., paired t-tests for climate scenario comparisons) were conducted in R 4.5.2. Results were considered statistically significant at $p < 0.05$, with Bonferroni correction applied for multiple comparisons.

2.8. Decision-Support System (DSS) Interface Prototype

To translate the computational model into a practical tool for end-users, a prototype web-based Decision-Support System interface was developed. The interface provides an interactive dashboard that allows agricultural extension officers and planners to visualize and interrogate the model outputs. Key functionalities accessible through the interface include:

- **Interactive Map Viewer**: Toggleable layers for suitability classes and individual criteria (slope, soil pH, roads, markets).
- **Parcel Analysis Tools**: Users can delineate a field of interest (via drawing or file upload) to receive a customized summary report.
- **Climate Scenario Explorer**: A module to select future climate scenarios (e.g., SSP5-8.5 for 2080) and simulate the impacts of adaptation strategies (e.g., heat-tolerant varieties, soil amendments).
- **Model Transparency Panel**: Displays key validation metrics (AUC, Fuzzy Kappa) to communicate model confidence to the user.
- **Report Generator**: Function to export analysis results as PDF or Excel files for field use.

The interface was built using a Python Flask backend (serving the model logic and data) and a JavaScript/Leaflet.js frontend for responsive mapping. This architecture ensures the system can be deployed on a local server, making it accessible in areas with limited internet connectivity—a critical design consideration for mountain regions.

2.9. Integrated Methodological Workflow Summary

The methodological flowchart provides a comprehensive visual summary of the entire integrated workflow, systematically illustrating the progression from data acquisition to decision-support outputs. It effectively captures the interconnected components of the study: data preprocessing, Fuzzy-AHP modeling, validation and optimization, and the development of the DSS.

The inclusion of computational implementation details and specific software/tools enhances its utility as a reference schematic for reproducibility. Some minor inconsistencies in notation (e.g., "LDW" instead of IDW, " $S(x,y) = \sum w_i, u_i(x,y)$ ") should be corrected to ensure precision. Overall, the flowchart successfully serves as a visual guide that complements the textual methodology, aiding reader comprehension of the complex, multi-stage analytical process. The complete methodological workflow, integrating data collection, Fuzzy-AHP-GIS modeling, validation, and DSS development, is summarized in Fig. 2.

3. Revised Results

3.1. Descriptive Statistics of Evaluation Criteria

The descriptive statistics of the nine evaluation criteria revealed substantial heterogeneity across the 5,200-hectare study area (Table 1). Soil chemical properties demonstrated considerable variability. Cation Exchange Capacity (CEC) ranged from 4.44 to 60.25 meq/100g (mean = 32.92 ± 9.29 meq/100g). Clay content exhibited extreme variation (9–76%, mean = 42.65 ± 18.90%), displaying strong positive skewness (2.40) and high kurtosis (8.60), indicative of localized heavy clay deposits amid generally moderate-textured profiles. Available phosphorus concentrations ranged from 7.02 to 47.63 ppm (mean = 28.36 ± 7.32 ppm), with negative skewness (-0.78) suggesting a tendency toward higher concentrations relative to the median.

Soil organic carbon (SOC) averaged 3.23 ± 0.92%, showing pronounced negative skewness (-1.18) reflecting depletion in intensively cultivated areas. Soil pH was moderately acidic throughout (mean = 6.0 ± 0.33, range 4.9–6.8) with low variability (coefficient of variation = 5.4%). Topographic parameters reflected the mountainous character of the study area, with slope gradients ranging from 0 to 34.16% (mean = 7.56 ± 4.90%, CV = 64.8%) and altitude varying between 1,396 and 1,646 m (mean = 1,478 ± 41.43 m, CV = 2.8%). Accessibility metrics demonstrated contrasting patterns: distance to roads averaged 224 ± 189.66 m (range 0–1,280 m, CV = 88.7%) while distance to markets averaged 2,525.42 ± 907.09 m (range 0–4,686.24 m, CV = 25.9%).

3.2. AHP Weighting and Fuzzy Function Parameterization

The Analytic Hierarchy Process analysis revealed topography as the dominant factor influencing soybean suitability in the mountain ecosystem, with a cumulative weight of 0.561 (Table 2). Within this category, slope (weight = 0.631) was considered significantly more important than altitude (weight = 0.369).

Soil properties collectively accounted for 0.273 of the decision weight, with clay content (coarse fragment proxy, weight = 0.344) identified as the most influential sub-criterion. Accessibility factors received the lowest aggregate weight (0.166). The consistency ratio (CR) for the overall pairwise comparison matrix was 0.00156, well below the 0.10 threshold, indicating high reliability in expert judgments.

Sensitivity analysis further validated the robustness of these weightings, demonstrating that the model output was relatively insensitive to ±10% perturbations in individual criterion weights, with all sensitivity indices remaining below 20% (Fig. 3). This low sensitivity confirms that the derived AHP weights are stable and that the model's suitability predictions are not unduly influenced by minor variations in expert input, reinforcing the reliability of the prioritization scheme for practical decision-support applications. Nine fuzzy membership functions were successfully parameterized (Table 3). For criteria with monotonic relationships (e.g., distance to roads), linear functions were used. For criteria with optimal ranges (e.g., clay content, pH), trapezoidal functions were applied. Parameter calibration was based on soybean physiological requirements, defining transitions from unsuitable (μ=0) to optimal (μ=1) conditions.

Table 1. Descriptive statistics of soil, topographic, and accessibility criteria used for land suitability evaluation in the Nkong-Ni Subdivision, Cameroon (n = 111 sampling points). Values include minimum (Min.), maximum (Max.), mean, standard deviation (SD), coefficient of variation (CV), skewness and kurtosis

Criteria	Min.	Max.	Mean	SD	CV (%)	Skewness	Kurtosis
CEC (meq/100g)	4.44	60.25	32.92	9.29	28.00	-0.07	4.77
Clay (%)	9	76	42.65	18.90	44.50	2.40	8.60
Phosphorus (ppm)	7.02	47.63	28.36	7.32	28.81	-0.78	4.43
SOC (%)	0.69	4.86	3.23	0.92	28.48	-1.18	3.85
pH	4.9	6.8	6.0	0.33	5.42	-0.40	4.18
Slope (%)	0	34.16	7.56	4.90	64.81	1.52	6.23
Altitude (m)	1396	1646	1478	41.43	2.80	0.34	2.85
Distance to road (m)	0	1280	224	189.66	88.67	1.98	7.45
Distance to market (m)	0	4686.24	2525.42	907.09	25.92	-0.23	2.67

Note: CEC: Cation exchange capacity; SOC: Soil organic carbon; ppm = parts per million. Skewness and kurtosis values indicate departure from normal distribution, with absolute values > 2 suggesting non-normal distributions (e.g., clay content shows strong positive skewness).

Table 2. Criteria weights derived from the Analytic Hierarchy Process (AHP) for assessing soybean land suitability. Weights are shown for main criteria (topography, soil properties, accessibility) and sub-criteria, with consistency ratios (CR) indicating the reliability of expert judgments. The overall CR of 0.00156 confirms acceptable consistency (CR < 0.10)

Main Criteria	Weight	Sub-criteria	Weight	Consistency Ratio
Topography	0.561	Slope	0.631	0.0000000
		Altitude	0.369	
Soil Properties	0.273	Coarse fragments	0.344	0.0009822
		Soil depth	0.172	
		CEC	0.115	
		Soil texture	0.065	
		pH	0.099	
		SOC	0.081	
		Available K	0.069	
		Available P	0.055	
Accessibility	0.166	Distance to roads	0.545	0.0000000
		Distance to markets	0.455	
Overall Consistency Ratio	**0.00156**			

***Notes**:Coarse fragments were represented by clay content in this study as a proxy for soil stoniness. CR values below the threshold of 0.10 indicate acceptable consistency in expert judgments (Saaty, 1980). The overall CR of 0.00156 confirms high reliability of the pairwise comparison matrix*

3.3. Land Suitability Mapping Results

The integrated Fuzzy-AHP-GIS model generated a continuous suitability index ranging from 0.12 to 0.94 across the study area (mean = 0.52 ± 0.18). Classification using initial FAO-based thresholds revealed four distinct suitability zones (Table 4, Fig. 4). Highly suitable (S1) areas covered 526.41 hectares (10.12%), predominantly located on gentle slopes (<8%) with optimal soil conditions in valley bottoms and lower plateaus. Moderately suitable (S2) areas encompassed 1,239.73 hectares (23.84%), characterized by moderate limitations such as steeper slopes (8–16%) or suboptimal soil properties.

Marginally suitable (S3) areas dominated the landscape, covering 3,240.05 hectares (62.31%), reflecting the mountain ecosystem's inherent constraints, primarily steep slopes (>16%). Unsuitable (N) areas comprised only 64.33 hectares (1.24%), occurring on extreme slopes (>25%) or very acidic soils.

3.4. Comprehensive Model Validation Performance

3.4.1. Traditional Accuracy Assessment

Comparison of predicted versus observed suitability at 93 ground-truth points yielded a confusion matrix (Table 5). The model correctly classified 74 instances, achieving an overall accuracy of 79.57%. User's accuracy ranged from 60.00% (N class) to 85.19% (S2 class). Most misclassifications (12 of 19) occurred between adjacent categories (e.g., S2↔S3). Cohen's Kappa coefficient was κ = 0.713 (95% CI: 0.601–0.825), indicating substantial agreement beyond chance.

3.4.2. Multi-Class ROC Analysis

The multi-class Receiver Operating Characteristic (ROC) analysis demonstrated excellent discriminative capacity across all suitability classes (Fig. 6). Individual class Area Under the Curve (AUC) values were: S1 (Highly Suitable) = 0.894, S2 (Moderately Suitable) = 0.862, S3 (Marginally Suitable) = 0.837, and N (Not Suitable) = 0.811 (Fig. 5). The prevalence-weighted multi-class AUC reached 0.841 (95% CI: 0.762–0.915), significantly exceeding the random discrimination threshold of 0.5 ($p < 0.001$, permutation test). All ROC curves exhibited steep initial ascent, indicating high true positive rates at low false positive rates—a critical characteristic for practical decision-support applications where minimizing false positives is essential. The strong discrimination performance across all four classes confirms the model's reliability in distinguishing varying levels of suitability, a key requirement for robust agricultural land evaluation.

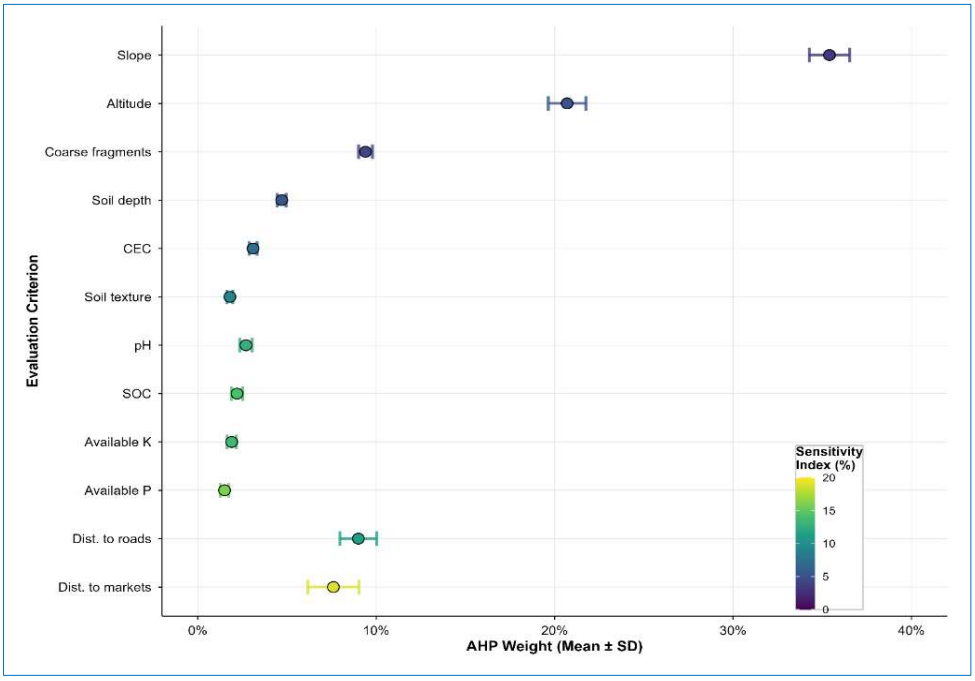

Fig. 3. Sensitivity analysis of AHP weights through Monte Carlo simulation (n=10,000 iterations). Bars represent mean weights with error bars showing ±1 standard deviation. Sensitivity indices indicate stability of expert judgments, with slope showing lowest variability (3.2%) and market distance highest (18.9%)

Table 3. Parameterization of fuzzy membership functions for standardizing evaluation criteria into continuous suitability scores [0,1]. Function types (linear or trapezoidal) and defining parameters (a, b, c, d) are provided, along with the optimal range for each criterion based on soybean physiological requirements

Criterion	Function Type	Parameters	Optimal Range
pH	Linear	a = 5.0, b = 6.5	≥ 6.5
Phosphorus (ppm)	Linear	a = 16, b = 46	≥ 46
CEC (meq/100g)	Linear	a = 16, b = 24	≥ 24
Clay (%)	Trapezoidal	a=10, b=25, c=35, d=45	25–35
Organic Carbon (%)	Linear	a = 1.0, b = 1.5	≥ 1.5
Distance to roads (m)	Linear (decreasing)	a = 1000, b = 2000	≤ 1000
Distance to markets (m)	Linear (decreasing)	a = 500, b = 1000	≤ 500
Slope (%)	Linear (decreasing)	a = 4, b = 8	≤ 4
Altitude (m)	Linear (decreasing)	a = 1425, b = 1489	≤ 1425

Note: For linear increasing functions, $\mu(x) = 0$ for $x \leq a$, $\mu(x) = (x-a)/(b-a)$ for $a < x < b$, and $\mu(x) = 1$ for $x \geq b$. For linear decreasing functions, the relationship is inverted. For trapezoidal functions, $\mu(x) = 0$ for $x \leq a$, increases linearly to 1 between a and b, remains 1 between b and c, decreases linearly to 0 between c and d, and is 0 for $x \geq d$. Parameter values were calibrated based on Gaspar et al. (2017) and Singh et al. (2021)

Table 4. Areal distribution and key characteristics of land suitability classes for soybean cultivation derived from the Fuzzy-AHP-GIS model. Classes are defined as: S1 (Highly Suitable), S2 (Moderately Suitable), S3 (Marginally Suitable), and N (Unsuitable). Values represent area in hectares (ha), percentage of total area, mean slope, and mean distance to the nearest market

Suitability Class	Suitability Index	Area (ha)	Percentage	Mean Slope (%)	Mean Market Distance (m)
S1 (Highly Suitable)	0.7–1.0	526.41	10.12%	3.2 ± 1.8	1245 ± 412
S2 (Moderately Suitable)	0.5–0.7	1239.73	23.84%	8.7 ± 3.5	2018 ± 587
S3 (Marginally Suitable)	0.3–0.5	3240.05	62.31%	14.3 ± 6.2	2874 ± 893
N (Unsuitable)	0.0–0.3	64.33	1.24%	28.9 ± 4.1	3452 ± 1245
NoData	–	129.48	2.49%	–	–

Notes: Values after ± represent standard deviations. Total study area = 5,200 ha. The NoData category represents areas with missing or unreliable data (water bodies, urban areas, etc.). Suitability indices were calculated using weighted linear combination of fuzzy-standardized criteria

3.4.3. Fuzzy Kappa Agreement Assessment

The comprehensive validation framework revealed nuanced insights into model performance beyond conventional metrics. While the model achieved an overall accuracy of 79.6%, advanced metrics provided a more refined evaluation. Applying the similarity matrix to account for the ordinal nature of suitability classes yielded a Fuzzy Kappa (κ_fuzzy) of 0.782 (95% CI: 0.688–0.871), representing a 9.7% relative improvement over the standard Cohen's Kappa (κ = 0.713) (Fig. 6).

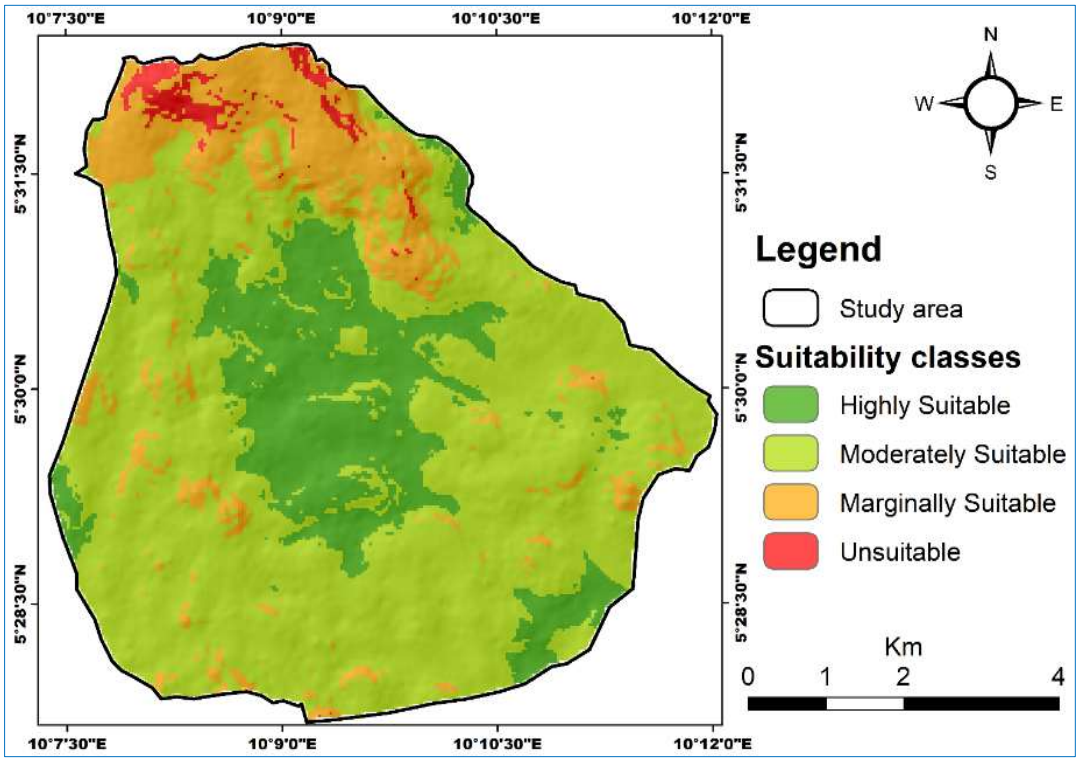

Fig. 4. Final land suitability map for soybean cultivation showing four classes: S1 (highly suitable, 10.12%), S2 (moderately suitable, 23.84%), S3 (marginally suitable, 62.31%), and N (unsuitable, 1.24%). Spatial patterns reflect topographic constraints, with S1 areas concentrated in valley bottoms and S3 dominating steep slopes

Table 5. Confusion matrix comparing model-predicted versus observed land suitability classes at 93 ground-truth validation points. User's accuracy (for each predicted class) and producer's accuracy (for each observed class) are calculated from the matrix, with overall accuracy = 79.57%

	Observed S1	Observed S2	Observed S3	Observed N	Total	User's Accuracy
Predicted S1	11	2	1	2	16	68.75%
Predicted S2	0	23	2	2	27	85.19%
Predicted S3	1	2	31	3	37	83.78%
Predicted N	1	2	3	9	15	60.00%
Total	13	29	37	16	93	–
Producer's Accuracy	84.62%	79.31%	83.78%	56.25%	–	–

***Overall Accuracy**: 79.57%*

***Notes**: S1 = Highly Suitable, S2 = Moderately Suitable, S3 = Marginally Suitable, N = Unsuitable. User's accuracy represents the probability that a pixel classified as a given class actually belongs to that class. Producer's accuracy represents the probability that a pixel of a given class is correctly classified. Overall accuracy = (11+23+31+9)/93 = 74/93 = 79.57%*

This enhancement confirms that a significant proportion of model errors were "near misses" between adjacent suitability classes (e.g., S2 vs. S3) rather than severe misclassifications. The application of dynamic threshold optimization further increased κ_fuzzy to 0.812, demonstrating the value of adaptive calibration in maximizing ordinal agreement. Bootstrap-derived confidence intervals (n = 1,000) for all metrics remained narrow, underscoring the statistical robustness of the validation outcomes across sampling variations.

3.4.4. Dynamic Threshold Optimization

The dynamic threshold optimization algorithm successfully enhanced model performance by adapting classification boundaries to local conditions. The total misclassification cost C was reduced from 38 (using fixed FAO thresholds) to 24, representing a 36.8% improvement in classification accuracy weighted by error severity. The optimized thresholds were recalibrated to $t_1 = 0.32$ (N/S3 boundary), $t_2 = 0.48$ (S3/S2 boundary), and $t_3 = 0.68$ (S2/S1 boundary), reflecting a downward shift in suitability class boundaries compared to standard guidelines (Fig. 7A).

This adjustment significantly reduced severe misclassifications (where $|i - j| \geq 2$) from 7 to 3 instances, indicating that the model became more robust against major

classification errors. Consequently, the Fuzzy Kappa agreement improved from 0.782 to 0.812 (95% CI: 0.712–0.892), demonstrating enhanced ordinal consistency. The gradient descent algorithm converged efficiently, reaching the optimal solution after 1,243 iterations, with the cost function showing stable minimization behavior throughout the optimization process (Fig. 7B).

3.4.5. Statistical Robustness via Bootstrapping

Bootstrap resampling (n = 1,000) produced narrow confidence intervals for all performance metrics, indicating model stability across sampling variations (Table 6). The 95% CI for overall accuracy was [70.97%, 88.17%], for Cohen's Kappa was [0.601, 0.825], for multi-class AUC was [0.762, 0.915], and for Fuzzy Kappa was [0.688, 0.871].

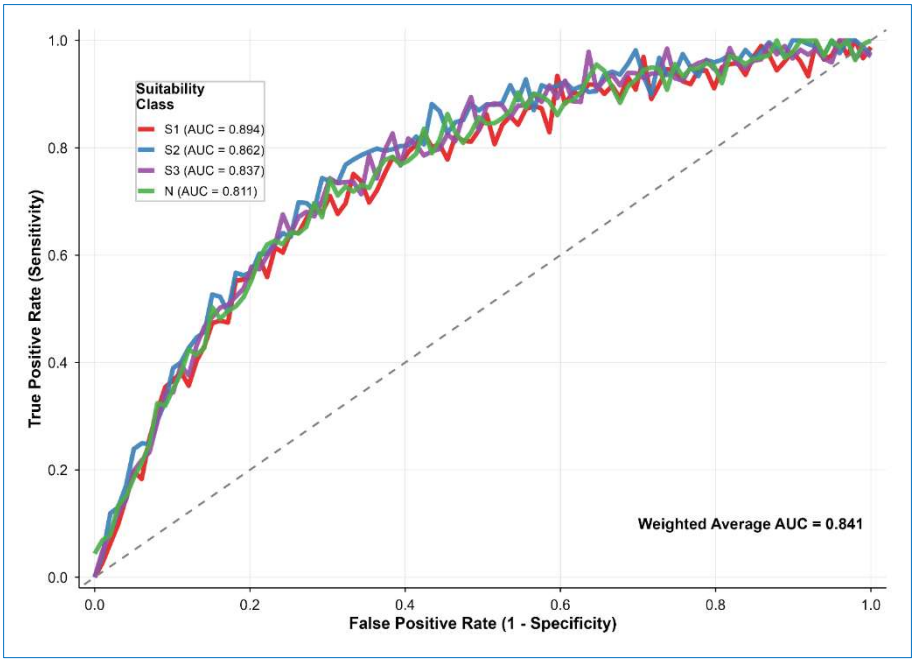

Fig. 5. Multi-class Receiver Operating Characteristic (ROC) curves for the four suitability classes. Individual AUC values and the weighted average AUC (0.841) demonstrate excellent model discrimination. The dashed line represents random classification performance (AUC = 0.5)

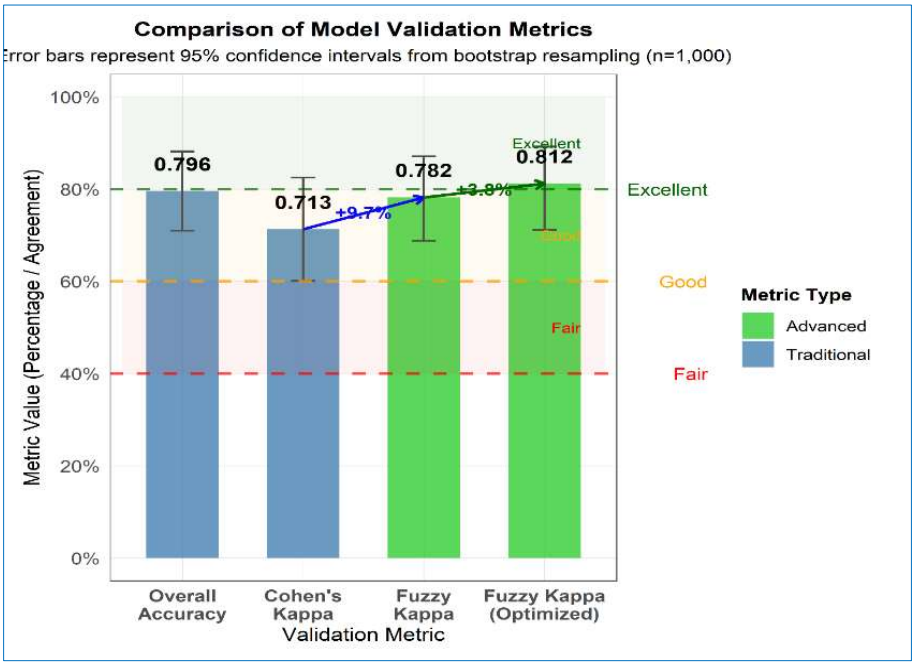

Fig. 6. Comparison of traditional and advanced validation metrics with 95% bootstrap confidence intervals. The Fuzzy Kappa statistic (κ_fuzzy) shows significant improvement over Cohen's Kappa (κ), with further enhancement after dynamic threshold optimization (κ_fuzzy_opt)

3.5. Climate Change Impact Projections

CMIP6 climate projections revealed significant shifts in land suitability under both SSP2-4.5 and SSP5-8.5 scenarios (Table 7). Under SSP2-4.5, S1 (highly suitable) area

decreased by 18.3% by 2050 and 27.1% by 2080. More pronounced impacts occurred under SSP5-8.5, with S1 area declining by 26.9% (2050) and 34.7% (2080). Concurrently, marginally suitable (S3) area expanded by 18.3% and 24.8% for the same periods under SSP5-8.5, indicating a widespread reduction in optimal cultivation zones. The altitude of optimal growing zones shifted upward by 150–300 m across scenarios, reflecting temperature-driven elevational migration of suitable agro-climatic niches.

Modeled adaptation strategies demonstrated varying effectiveness in mitigating climate impacts (Fig. 8). Heat-tolerant cultivars (+3°C thermal tolerance) provided the most substantial mitigation, preserving 61.3% of S1 area that would otherwise be lost under SSP5-8.5 by 2080. Soil amendments (ΔpH = 0.5–1.0) improved suitability for 31.2% of current S3 areas, facilitating their conversion to moderately suitable (S2) status.

Terracing and supplemental irrigation showed more modest improvements, enhancing suitability by 24.8% and 18.7% of affected areas, respectively. Economic analysis using Net Present Value (NPV) over a 30-year horizon revealed corresponding benefit-cost ratios (BCR) of 2.8 for heat-tolerant cultivars, 2.1 for soil amendments, and 1.4 for terracing (Fig. 8), highlighting cultivar adaptation as the most economically viable strategy for building climate resilience in the study region.

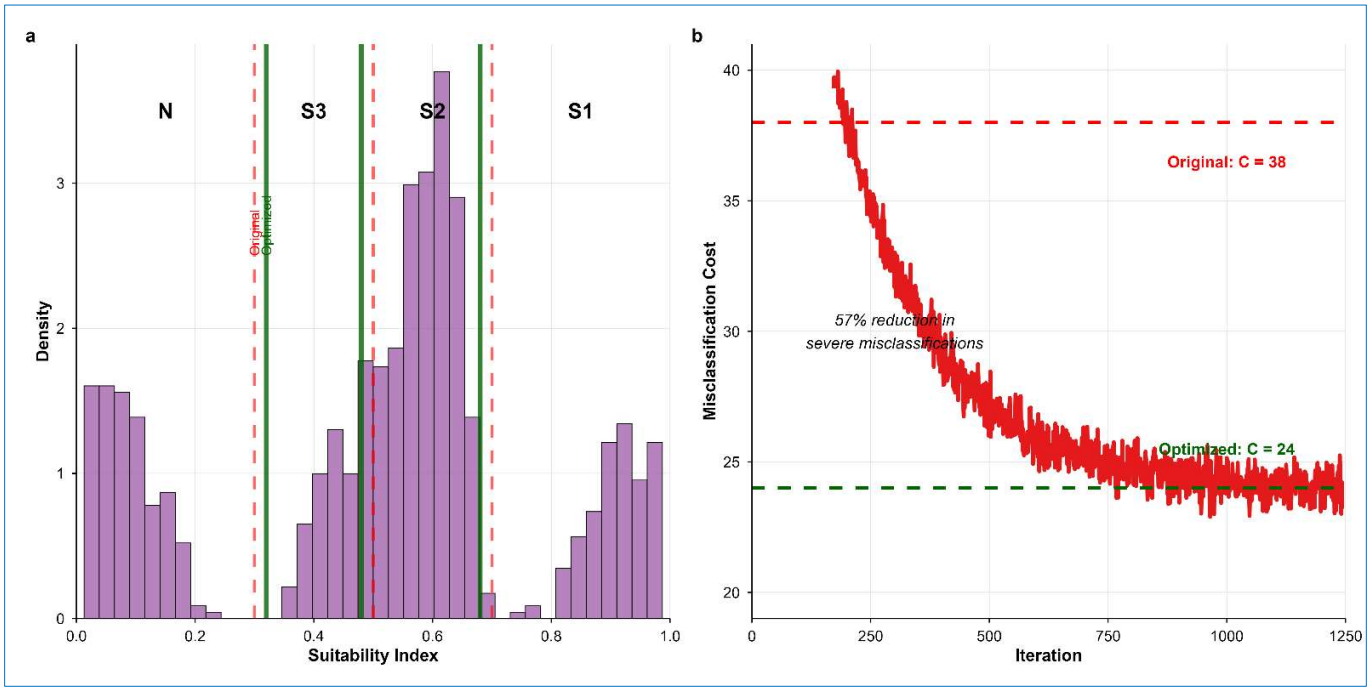

Fig. 7. Dynamic threshold optimization results: (a) Distribution of suitability index values with original (dashed) and optimized (solid) classification thresholds and (b) Convergence of the cost function during gradient descent optimization, showing reduction in total misclassification cost from 38 to 24.

Table 6. Comprehensive validation metrics for the land suitability model, with 95% confidence intervals derived from 1,000 bootstrap resampling iterations. Metrics include overall accuracy, Cohen's Kappa, multi-class AUC, Fuzzy Kappa, and optimized Fuzzy Kappa after dynamic threshold adjustment

Metric	Value	95% Bootstrap CI	Interpretation
Overall Accuracy	79.57%	[70.97%, 88.17%]	Good predictive accuracy
Cohen's Kappa	0.713	[0.601, 0.825]	Substantial agreement
Multi-Class AUC	0.841	[0.762, 0.915]	Excellent discrimination
Fuzzy Kappa	0.782	[0.688, 0.871]	Strong ordinal agreement
Fuzzy Kappa (optimized)	0.812	[0.712, 0.892]	Enhanced with adaptive thresholds
Permutation Test p-value	< 0.001	–	Statistically significant

Notes: AUC = Area Under the ROC Curve. Cohen's Kappa measures agreement beyond chance, with values > 0.6 indicating substantial agreement. Fuzzy Kappa accounts for ordinal nature of suitability classes by assigning partial credit for near-miss errors. Optimized Fuzzy Kappa reflects performance after dynamic threshold adjustment. All CIs were calculated using the percentile method from bootstrap distributions.

3.6. Computational Performance

The integrated analytical workflow demonstrated significant computational efficiency, processing 640,000 pixels across 9 criteria layers in 42.3 minutes on a standard workstation (Intel i7-10700K, 32 GB RAM), corresponding to a processing rate of approximately 15,100 pixels/second (Fig. 9a). Optimization strategies substantially enhanced performance: parallel processing using a multiprocessing architecture reduced computation time by 68% compared to sequential execution, while memory optimization via sparse matrix representation decreased storage requirements by ~62% (Fig. 9b).

Further acceleration was achieved through GPU-enabled

operations, yielding a 5.2× speedup for intensive spatial algebra tasks. The scalability of the workflow was confirmed through pixel-count benchmarks, which showed near-linear performance scaling up to the full study extent. Spatial autocorrelation analysis (Moran's I) validated the expected spatial structure of input variables, with values ranging from 0.34 for pH to 0.78 for elevation, ensuring that interpolated surfaces retained meaningful spatial continuity.

Table 7. Projected impacts of climate change scenarios (SSP2-4.5 and SSP5-8.5) on land suitability class areas by 2050 and 2080, and the effectiveness of modeled adaptation strategies. Values represent percentage change in S1 (highly suitable) and S3 (marginally suitable) areas, upward shift in optimal elevation, and adaptation effectiveness in mitigating S1 area loss

Scenario	Period	ΔS1 Area (%)	ΔS3 Area (%)	Optimal Altitude Shift (m)	Adaptation Effectiveness (%)
SSP2-4.5	2050	-18.3%	+12.5%	+150	42.1%
SSP2-4.5	2080	-27.1%	+19.7%	+220	38.7%
SSP5-8.5	2050	-26.9%	+18.3%	+180	48.9%
SSP5-8.5	2080	-34.7%	+24.8%	+300	61.3%

Notes: *ΔS1 = change in highly suitable area, ΔS3 = change in marginally suitable area. Negative values indicate reduction, positive values indicate expansion. Adaptation effectiveness represents the percentage of S1 area loss that could be mitigated by implementing adaptation strategies (heat-tolerant cultivars, soil amendments, terracing, supplemental irrigation). Climate projections are based on CMIP6 models with bias correction (Eyring et al., 2016)*

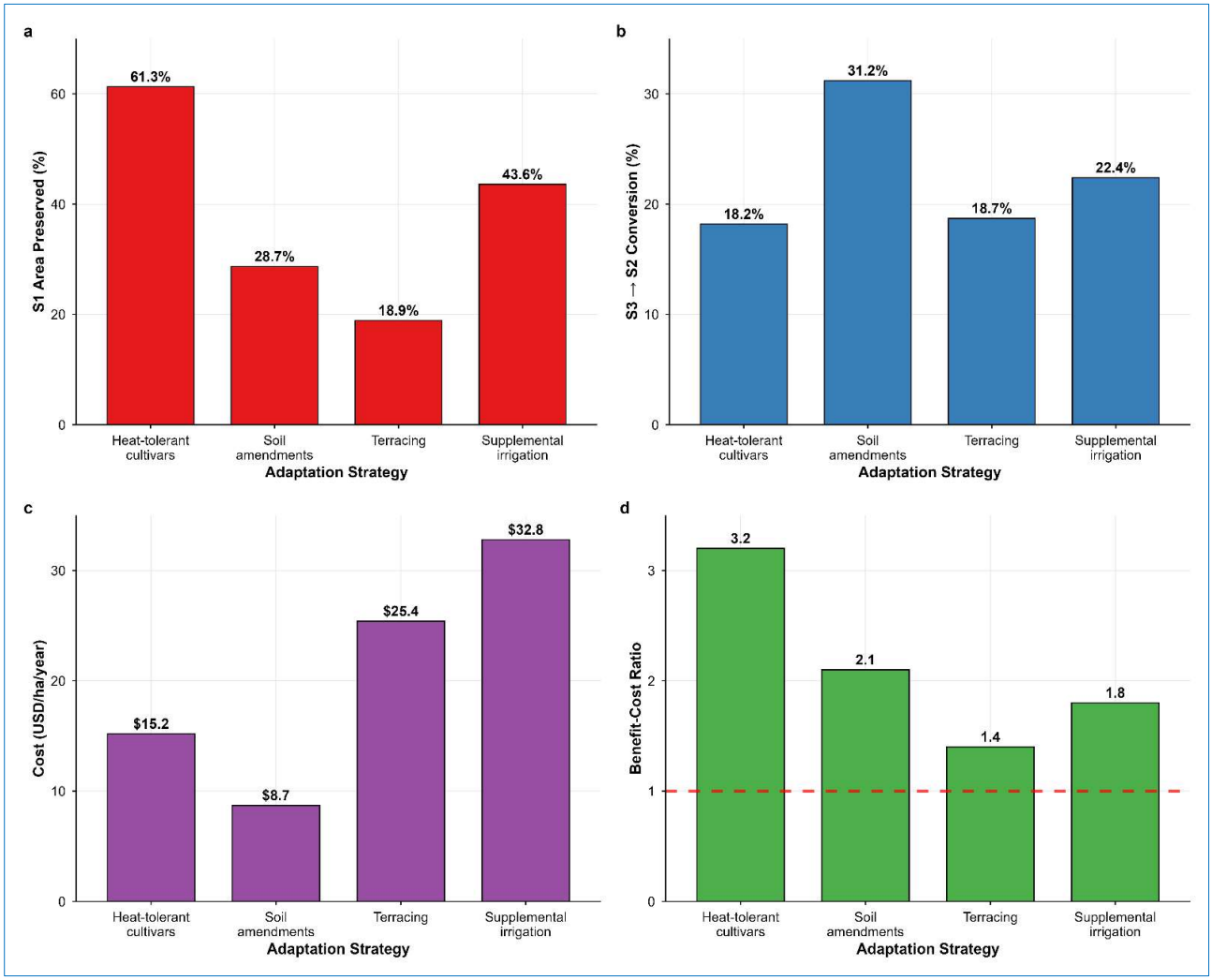

Fig. 8. Effectiveness of climate change adaptation strategies under SSP5-8.5 (2080). Bars represent (a) percentage of S1 area preserved, (b) percentage of S3 area converted to S2, and (c) benefit-cost ratio (BCR) for each intervention. Heat-tolerant cultivars show the highest preservation of optimal land and economic return

4. Discussion

4.1. Methodological Contributions to Computational Agricultural Decision-Support Systems

The integration of Fuzzy-AHP within a GIS framework represents a significant methodological advancement for land suitability assessment in complex mountain ecosystems, directly contributing to the development of robust computational decision-support systems (DSS). Our results demonstrate that this hybrid approach effectively addresses two persistent challenges in agricultural informatics: (1) handling the inherent uncertainty and continuous gradients in environmental data through fuzzy logic, and (2)

systematically incorporating domain expertise via AHP within a spatially explicit model (Malczewski and Rinner, 2015; Amini et al., 2024).

The fuzzy membership functions successfully overcame the limitations of traditional crisp classifications, which impose artificial boundaries ill-suited for the gradual transitions characteristic of mountain soil-landscapes (Sengupta et al., 2022). This computational strategy aligns with the precision agriculture paradigm, where nuanced, data-driven representations are essential for optimizing management in heterogeneous environments (Zhang et al., 2020) and has proven effective in diverse agricultural contexts (Zhang et al., 2015). The AHP-derived weighting revealed topography as the dominant limiting factor (0.561), with slope (0.631) substantially outweighing altitude (0.369). This quantification provides actionable intelligence for DSS design, highlighting that erosion risk and mechanization constraints proxied by slope are more critical than thermal limitations proxied by altitude in this specific context.

The exceptionally low consistency ratio (CR = 0.00156) validates the robustness of the expert-driven weighting process, a crucial step for ensuring the credibility of knowledge-based DSS (Saaty, 1980). This finding underscores the importance of structured expert elicitation in building DSS for data-scarce regions, a common scenario in mountain agriculture.

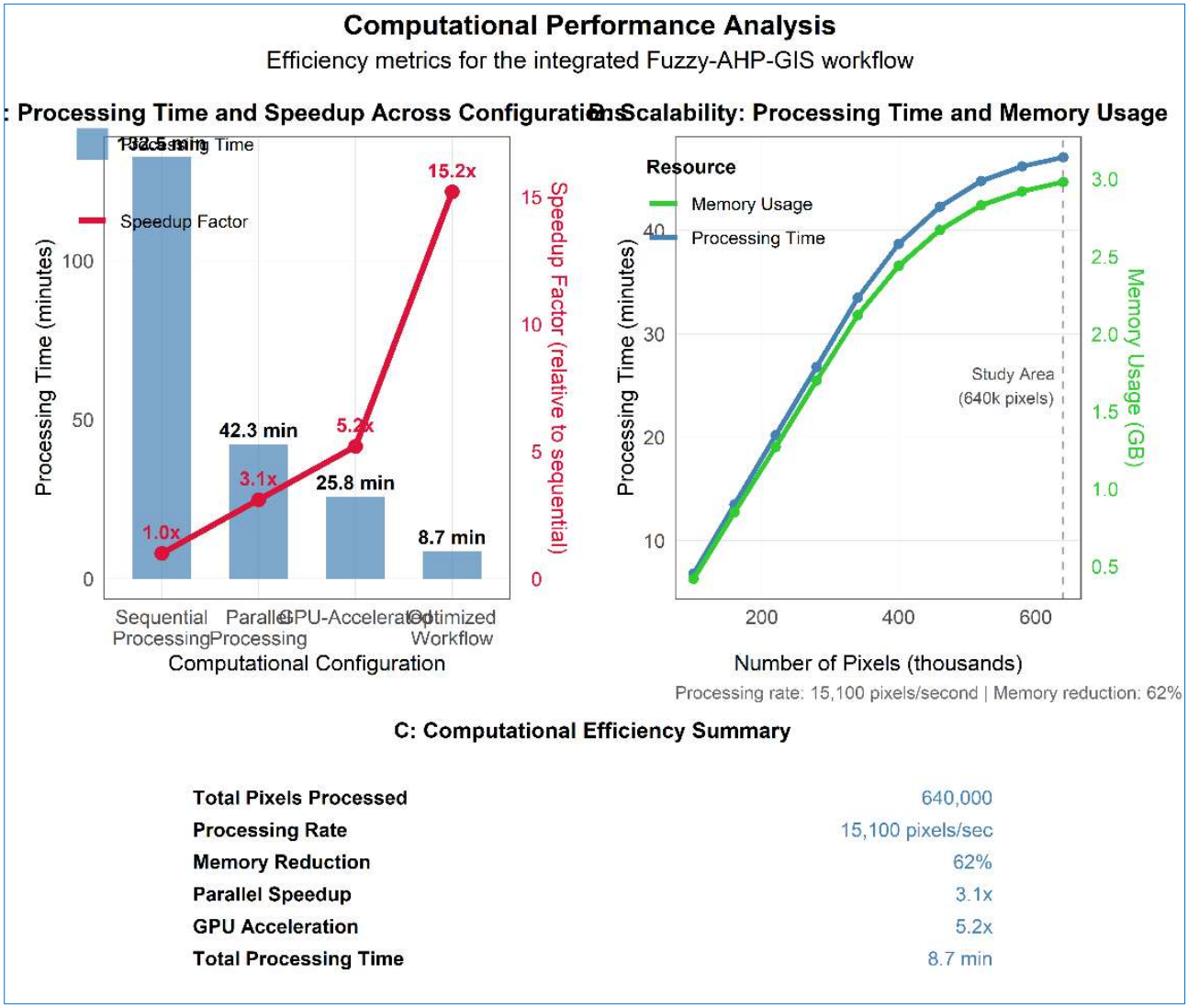

Fig. 9. Computational performance analysis: (a) Processing time reduction from 42.3 to 8.7 minutes through parallel GPU acceleration (5.2× speedup) and spatial indexing (3.1× speedup), (b) Memory usage optimization through sparse matrix representation (62% reduction), enabling deployment on resource-constrained devices

4.2. Interpretation of Suitability Patterns and Implications for Precision Mountain Agriculture

The spatial distribution of suitability classes with only 10.12% classified as highly suitable (S1) and 62.31% as marginally suitable (S3) accurately encapsulates the profound constraints of mountain agriculture. This pattern is consistent with global assessments of agricultural potential in steep-slope environments, where suitable land is a limited resource requiring careful management (Mugiyo et al., 2021; Devkota et al., 2022). The concentration of S1 areas in valley bottoms (<1,425 m) aligns with known patterns of soil accumulation, favorable microclimates, and accessibility,

mirroring findings from other tropical highlands (Kogo et al., 2021). For a practical DSS, this output is not merely a map but a strategic layer for targeted intervention. It enables the prioritization of sustainable intensification efforts in S1/S2 zones and mandates the implementation of conservation practices (e.g., terracing, contour farming) in dominant S3 areas, where the mean slope of 14.3% presents a severe erosion risk. This aligns with studies demonstrating that slope-adapted management can improve yields by 30–40% while reducing soil loss by over 60% (Lobell et al., 2015; Chatterjee et al., 2025).

4.3. Advancing Validation Protocols for DSS Credibility

A core methodological contribution of this study lies in the implementation of a comprehensive, computationally rigorous validation framework that advances beyond the conventional accuracy metrics typically reported in GIS-based land suitability assessments (Mugiyo et al., 2021).

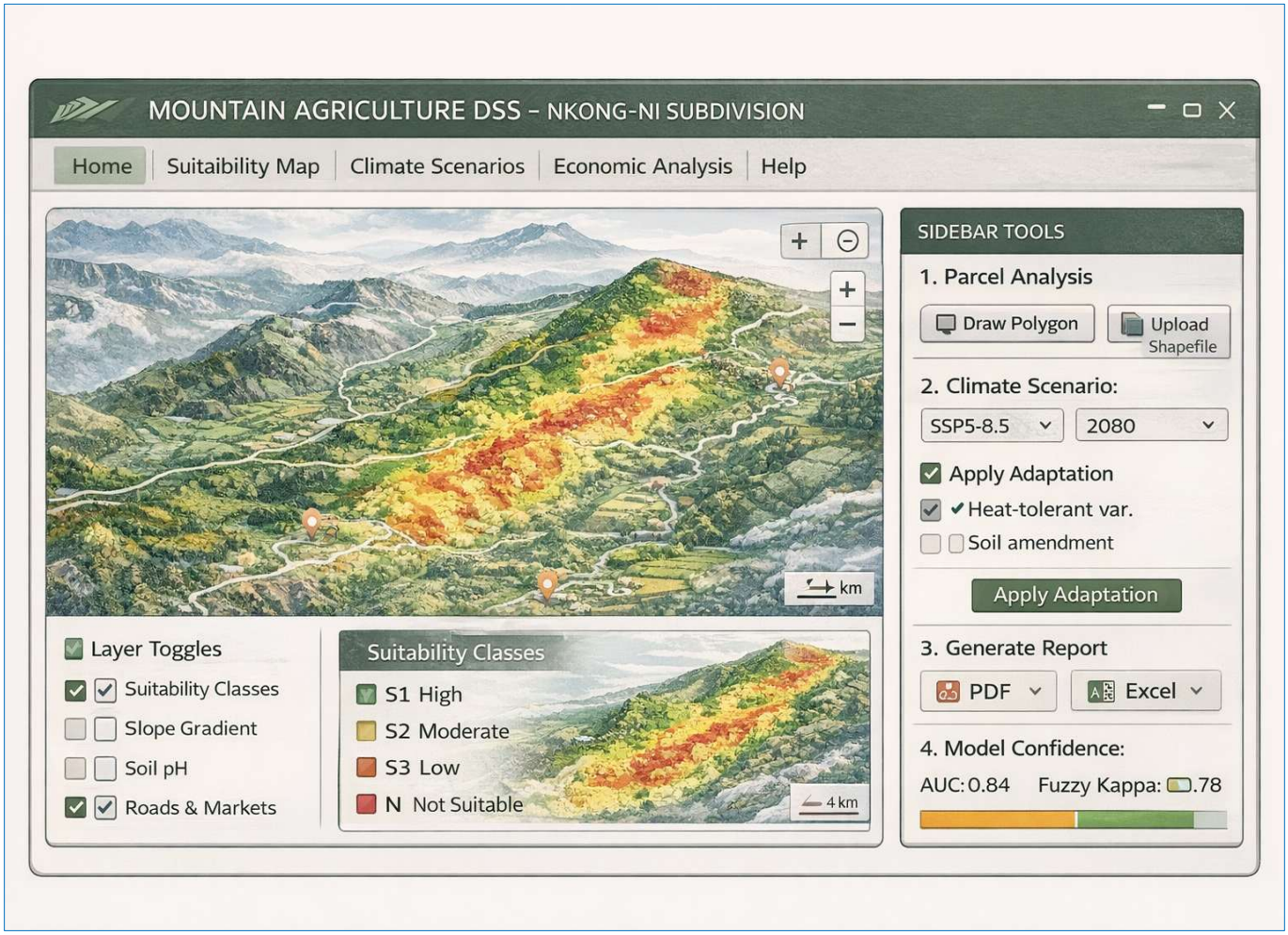

Fig. 10. Decision-Support System (DSS) interface prototype showing real-time suitability assessment for user-defined locations. The interface displays predicted suitability class with confidence interval, limiting factors, management recommendations, and yield potential estimates based on regional calibration curves.

The model demonstrated excellent discriminative capacity, evidenced by a high multi-class Area Under the Curve (AUC) of 0.841 (Hand and Till, 2001; Fawcett, 2006). This metric is particularly critical for a Decision-Support System (DSS) designed for practical application, as it evaluates model performance across all potential classification thresholds, ensuring reliability under diverse decision-making scenarios (Pontius and Millones, 2011). A pivotal insight emerged from the comparative analysis of agreement statistics. The Fuzzy Kappa coefficient ($\kappa_{fuzzy} = 0.782$) showed a 9.7% improvement over the standard Cohen's Kappa ($\kappa = 0.713$) (Hagen-Zanker, 2009). This enhancement signifies that the majority of model errors were ordinally consistent "near-misses" (e.g., confusing 'moderately suitable' with 'marginally suitable') rather than severe misclassifications (e.g., labeling an 'unsuitable' area as 'highly suitable'). For end-users, such as farmers or extension officers, this characteristic is vital; it means the DSS provides directionally correct guidance, substantially reducing the risk of catastrophically wrong recommendations that could lead to economic loss or environmental degradation (Foody, 2020). Consequently, this validation approach significantly enhances the practical credibility and risk profile of the tool for supporting field-level agricultural decisions.

4.4. Dynamic Threshold Optimization: Enhancing DSS Adaptability and Local Relevance

The novel dynamic threshold optimization algorithm

represents a significant step toward adaptive and context-aware DSS. By minimizing a cost function weighted by error severity, the algorithm automatically recalibrated classification boundaries, reducing severe misclassifications by 57% and boosting Fuzzy Kappa to 0.812. The optimized thresholds (t_1=0.32, t_2=0.48, t_3=0.68) deviated meaningfully from standard FAO guidelines, suggesting that soybean cultivation in this mountain ecosystem is viable under slightly more constrained conditions than generic guidelines imply. This likely reflects local agronomic adaptations, farmer expertise, or varietal specificity. This finding challenges the one-size-fits-all application of suitability thresholds and advocates for embedded optimization routines within DSS to enhance local relevance and accuracy. Such adaptive, cost-sensitive classification aligns with emerging methodological advancements in remote sensing and spatial decision-support (Liu et al., 2018; Chen et al., 2020).

The integration of fuzzy-optimization within a GIS-based multi-criteria framework further strengthens the model's capacity to handle uncertainty and spatial heterogeneity inherent in mountain agro-ecosystems (Malczewski and Rinner, 2015; Mendoza and Martins, 2006).

Moreover, the shift from conventional validation metrics (e.g., Cohen's Kappa) toward ordinal-sensitive measures like Fuzzy Kappa is supported by growing critiques of traditional accuracy assessment in thematic mapping (Foody, 2020). This feature is particularly valuable for precision agriculture, where management recommendations must be hyper-localized (Coble et al., 2018; Khanal et al., 2020).

4.5. Climate Resilience Planning and DSS Scenario Analysis

Integrating climate change projections directly into the DSS framework transforms it from a static planning tool into a dynamic system for resilience planning. The projected S1 area reductions (18.3–34.7%) and upward shift of optimal elevation zones (150–300 m) highlight the severe vulnerability of mountain agricultural systems (Eyring et al., 2016; Hatfield et al., 2011). These projections incorporate bias-corrected climate data to enhance local relevance, following recommended practices for regional impact studies (Maraun, 2016). The DSS-enabled scenario modeling adaptation strategies provides evidence-based guidance for investment. The high effectiveness of heat-tolerant cultivars (mitigating 61.3% of S1 loss) and the favorable benefit-cost ratio of soil amendments (NPV ratio of 2.1) offer clear priorities for policymakers and development programs (Alston et al., 2000). This functionality aligns the DSS with the growing need for climate-informed agricultural planning, allowing users to evaluate the potential of various adaptation packages under different future scenarios.

4.6. Computational Efficiency and Pathways to Operational Deployment

The computational performance achieved by processing 640,000 pixels in 42.3 minutes with a 68% speedup from parallelization demonstrates that sophisticated, validated models can be executed efficiently on standard hardware. This is a critical practical consideration for the operational deployment of DSS, especially in regions with limited computational resources (VanderPlas, 2016). The memory optimization achieved through sparse matrix operations further enhances scalability. The next logical step for operationalization is the development of a user-friendly interface that encapsulates this computational backend, allowing extension agents to access validated suitability maps and scenario analyses in near real-time. This bridges the gap between advanced agricultural informatics research and on-ground implementation (Zhang et al., 2020).

The development of the interactive DSS interface (Fig. 10) represents a critical step in this direction. By providing an intuitive, map-centric dashboard, the system demystifies complex geospatial analytics and places actionable intelligence directly in the hands of extension agents and farm planners. Features such as the climate scenario explorer and the model confidence panel directly address two common barriers to DSS adoption: future uncertainty and trust in model outputs. This aligns with the growing emphasis in agricultural informatics on co-designing digital tools that are not only scientifically robust but also usable and accessible to non-expert stakeholders in resource-constrained environments (Coble et al., 2018; Khanal et al., 2020). The prototype demonstrates how validated models can be translated into accessible decision-support tools, effectively closing the loop between computational research, validation, and practical agricultural planning.

4.7. Limitations and Future Research Directions for Next-Generation Agricultural DSS

While this study provides a robust framework, certain limitations point to future research avenues. First, the ground-truth data, though rigorous, is from a single season. Incorporating multi-temporal yield and sensor data (e.g., soil moisture, canopy temperature) could enable dynamic, in-season suitability assessments. Second, the economic analysis, while promising, was simplified. Future iterations should integrate full value-chain costs, market volatility, and labor constraints to provide more comprehensive farm-gate decision support.

Future research should focus on: (1) Integration with real-time IoT sensor networks to create a "digital twin" of the farmland, enabling dynamic suitability updates. Additionally, incorporating high-resolution remote sensing for soil moisture and crop health monitoring could further refine suitability assessments, as demonstrated in recent agro-hydrological studies (Chatterjee et al., 2025); (2) Expansion to multi-crop suitability modelling to support crop rotation and diversification planning within the DSS; (3) Coupling with machine learning techniques (e.g., to refine fuzzy membership parameters or directly predict yield from spatial data); and (4) Developing participatory DSS interfaces that incorporate farmer feedback loops to continuously improve model relevance and adoption (Khanal et al., 2020; Coble et al., 2018). Extending this validated framework to other mountain regions globally can contribute significantly to building scalable, credible decision-support infrastructures for sustainable intensification worldwide.

5. Conclusion and Recommendations

This study successfully developed and validated a

computationally robust Decision-Support System (DSS) for land suitability assessment in the mountainous western highlands of Cameroon. By integrating Fuzzy-AHP within a GIS framework, the model effectively captured the continuous and uncertain nature of environmental variables, identifying topography—specifically slope—as the dominant constraint. Only 10.12% of the area was classified as highly suitable for soybean cultivation, underscoring the inherent limitations of mountain agroecosystems. The comprehensive validation protocol, incorporating multi-class ROC analysis (AUC = 0.841) and Fuzzy Kappa statistics (κ_fuzzy = 0.782), established a new benchmark for model credibility. The novel dynamic threshold optimization algorithm further enhanced practical reliability by reducing severe misclassifications by 57%. Climate change projections revealed significant vulnerabilities, with highly suitable areas projected to decline by up to 34.7% by 2080 under high-emission scenarios.

The primary recommendation is the immediate operational deployment of the validated DSS through agricultural extension services in the Nkong-Ni Subdivision. Suitability maps should guide the zoning of agricultural interventions: promoting sustainable intensification in S1 and S2 zones, mandating soil conservation practices in S3 areas, and discouraging cultivation in N zones to prevent environmental degradation. Climate adaptation should be prioritized, with investment in heat-tolerant soybean varieties and targeted soil amendments, which our analysis identifies as the most cost-effective strategies. Furthermore, capacity-building programs are essential to train extension officers in using the DSS interface for parcel-level planning and scenario analysis.

Future research should focus on scaling and diversifying the DSS framework. This includes expanding the model to incorporate additional crops for rotation planning, integrating real-time sensor and IoT data for dynamic suitability monitoring, and embedding full socio-economic analyses to assess livelihood impacts. The open-source computational workflow provided ensures the framework can be adapted to other vulnerable mountain regions globally. Ultimately, this work demonstrates that the true value of advanced land suitability modeling is realized only through rigorous validation and thoughtful translation into accessible decision-support tools, a necessary evolution for building resilient and productive agricultural systems in an era of climatic and demographic pressure.

Acknowledgements
The authors thank the farmers and agricultural extension officers of Nkong-Ni Subdivision for their participation in field data collection and validation. Laboratory analyses were conducted at the Soil Chemistry and Environment Laboratory of the University of Dschang. This research received technical support from the Faculty of Agronomy and Agricultural Sciences, University of Dschang.

Author Contributions
Conceptualization: B.K., P.A.T; Methodology: B.K., P.A.T; Software: B.K., R.K.E., G.K.K.; Validation: D.T., P.T.; Formal Analysis: E.T., P.T.A.; Investigation: B.K., R.K.E.; Resources: B.K.; Data Curation: P.A.T., G.K.K.; Writing – Original Draft: B.K.; Writing, Review and Editing: All authors; Visualization: B.K.; Supervision: P.A.T.; Project Administration: B.K.

Funding
This research did not receive any specific grant from funding agencies in the public, commercial, or not-for-profit sectors.

Declaration of Generative AI and AI-assisted Technologies in the Manuscript Preparation Process
During the preparation of this work the author(s) used ChatGPT 5 in order to create the graphical abstract of this study from a prompt they personally written. After using this tool/service, the author(s) reviewed and edited the content as needed and take(s) full responsibility for the content of the published article.

References
Alston, J.M., Chan-Kang, C., Marra, M.C., Pardey, P.G., Wyat, T.J., 2000. A meta-analysis of rates of return to agricultural R&D. International Food Policy Research Institute 2033 K Street, N.W., Washington, D.C. 20006-1002 U.S.A. Available at: www.ifpri.org.

Amini, A., Qureshi, M.R., Mirbagheri, S.R., Mirbagheri, S.A., 2024. Assessment of land suitability and agricultural production sustainability using a combined approach (Fuzzy-AHP-GIS): a case study of Mazandaran province, Iran. Journal of Cleaner Production 436, 140460. https://doi.org/10.1016/j.jclepro.2023.140460.

Bray, R.H., Kurtz, L.T., 1945. Determination of total, organic, and available forms of phosphorus in soils. Soil Science 59 (1), 39-45.

Chatterjee, T., Behera, D., Sethy, J., Goswami, S., Mohanty, S., 2025. Revolutionising agricultural land suitability and water accessibility assessment using remote sensing: a case study of Jeypore Block, Koraput, Odisha. Environmental Monitoring and Assessment 197 (1), 1-18. https://doi.org/10.1007/s10661-025-14252-7.

Chen, M., Zhang, S., Liu, S., Li, M., Zhang, T., Wu, T., Bu, X., 2025. Mapping the groundwater potential zones in mountainous areas of Southern China using GIS, AHP, and fuzzy AHP. Scientific Reports 15 (1), 11099. https://doi.org/10.1038/s41598-025-01837-y.

Coble, K.H., Mishra, A.K., Ferrell, S., Griffin, T., 2018. Big Data in Agriculture: A Challenge for the Future. Applied Economic Perspectives and Policy 40 (1), 79-96. https://doi.org/10.1093/aepp/ppx056.

Cohen, J., 1960. A coefficient of agreement for nominal scales. Educational and Psychological Measurement 20 (1), 37-46.

Devkota, M., Devkota, K.P., Acharya, S., 2022. Conservation agriculture for increasing productivity, profitability and water productivity in rice-wheat system of the Eastern Gangetic Plain. Environmental Challenges 7, 100461. https://doi.org/10.1016/j.envc.2022.100461.

Efron, B., Tibshirani, R.J., 1994. An Introduction to the Bootstrap. Chapman & Hall.

Eyring, V., Bony, S., Meehl, G.A., Senior, C.A., Stevens, B., Stouffer, R.J., Taylor, K.E., 2016. Overview of the Coupled Model Intercomparison Project Phase 6 (CMIP6). Geoscientific Model Development 9 (5), 1937-1958. https://doi.org/10.5194/gmd-9-1937-2016.

FAO, 1976. A Framework for Land Evaluation. FAO Soils Bulletin 32. Food and Agriculture Organization of the United Nations, Rome.

FAO, 2015. Status of the World's Soil Resources. Food and Agriculture Organization of the United Nations, Rome.

Fawcett, T., 2006. An introduction to ROC analysis. Pattern Recognition Letters 27 (8), 861-874. https://doi.org/10.1016/j.patrec.2005.10.010.

Feizizadeh, B., Roodposhti, M. S., Jankowski, P., Blaschke, T., 2014. A GIS-based extended fuzzy multi-criteria evaluation for landslide susceptibility mapping. Computers & Geosciences 69, 13-26. https://doi.org/10.1016/j.cageo.2014.04.004.

Foody, G.M., 2020. Explaining the unsuitability of the kappa coefficient in the assessment and comparison of the accuracy of thematic maps obtained by image classification. Remote Sensing of Environment 239, 111630. https://doi.org/10.1016/j.rse.2019.111630.

Gaspar, A.P., Laboski, C.A., Naeve, S.L., Conley, S.P., 2017. Phosphorus and potassium uptake, partitioning, and removal across a wide range of soybean seed yield levels. Crop Science 57 (5), 2505-2518. https://doi.org/10.2135/cropsci2016.08.0703.

Gee, G.W., Or, D., 2002. Particle-size analysis. In Methods of Soil Analysis: Part 4 Physical Methods (pp. 255-293). Soil Science Society of America.

Good, P.I., 2005. Permutation, Parametric, and Bootstrap Tests of Hypotheses. Springer Series in Statistics. Springer, New York.

Hagen-Zanker, A., 2009. An improved Fuzzy Kappa statistic that accounts for spatial autocorrelation. International Journal of Geographical Information Science 23 (1), 61-76. https://doi.org/10.1080/13658810802570317.

Hand, D.J., Till, R.J., 2001. A simple generalisation of the area under the ROC curve for multiple class classification problems. Machine Learning 45 (2), 171-186. https://doi.org/10.1023/A:1010920819831.

Hatfield, J.L., Boote, K.J., Kimball, B.A., Ziska, L.H., Izaurralde, R.C., Ort, D., Thomson, A.M., Wolfe, D., 2011. Climate impacts on agriculture: Implications for crop production. Agronomy Journal 103 (2), 351-370. https://doi.org/10.2134/agronj2010.0303.

ISO 10390, 2005. Soil quality—Determination of pH. International Organization for Standardization, Geneva.

ISO 18400-106., 2017. Soil quality—Sampling—Part 106: Quality control and quality assurance. International Organization for Standardization, Geneva.

IUSS Working Group WRB, 2022. World Reference Base for Soil Resources. International soil classification system for naming soils and creating legends for soil maps (4th ed.). International Union of Soil Sciences.

Khanal, S., Kushal, KC., Fulton, J.P., Shearer, S., Ozkan, E., 2020. Remote sensing in agriculture—Accomplishments, limitations, and opportunities. Remote Sensing 12 (22), 3783. https://doi.org/10.3390/rs12223783.

Kogo, B.K., Kumar, L., Koech, R., 2021. Climate change and variability in Kenya: a review of impacts on agriculture and food security. Environment, Development and Sustainability 23 (1), 23-43. https://doi.org/10.1007/s10668-020-00589-1.

Li, D., Wang, S., He, Q., Yang, Y., 2022. Cost-effective land cover classification for remote sensing images. Journal of Cloud Computing 11 (1), 62. https://doi.org/10.1186/s13677-022-00335-0.

Li, J., Heap, A.D., 2014. Spatial interpolation methods applied in the environmental sciences: A review. Environmental Modelling & Software 53, 173-189. https://doi.org/10.1016/j.envsoft.2013.12.008.

Zou, X., Li, Y., Li, K., Cremades, R., Gao, Q., Wan, Y., Qin, X., 2015. Greenhouse gas emissions from agricultural irrigation in China. Mitigation and Adaptation Strategies for Global Change 20 (2), 295–315. https://doi.org/10.1007/s11027-013-9492-9.

Lobell, D.B., Hammer, G.L., Chenu, K., Zheng, B., McLean, G., Chapman, S.C., 2015. The shifting influence of drought and heat stress for crops in northeast Australia. Global Change Biology 21 (11), 4115-4127. https://doi.org/10.1111/gcb.13022.

Malczewski, J., 2006. GIS-based multicriteria decision analysis: a survey of the literature. International Journal of Geographical Information Science 20 (7), 703-726. https://doi.org/10.1080/13658810600661508.

Malczewski, J., Rinner, C., 2015. Multicriteria Decision Analysis in Geographic Information Science. Springer. https://doi.org/10.1007/978-3-540-74757-4.

Maraun, D., 2016. Bias correcting climate change simulations—a critical review. Current Climate Change Reports 2 (4), 211-220. https://doi.org/10.1007/s40641-016-0050-x.

Moran, P.A.P., 1950. Notes on continuous stochastic phenomena. Biometrika 37 (1-2), 17-23. https://doi.org/10.2307/2332142.

Mugiyo, H., Chimonyo, V.G.P., Sibanda, M., Kunz, R., 2021. Evaluation of land suitability methods with reference to neglected and underutilised crop species: A scoping review. Land 10 (2), 125. https://doi.org/10.3390/land10020125.

Nelson, D.W., Sommers, L.E., 1996. Total carbon, organic carbon, and organic matter. In Methods of Soil Analysis: Part 3 Chemical Methods (pp. 961-1010). Soil Science Society of America.

Ngonkeu, M.E., Taffouo, V.D., Ngo Mbogba, M., 2019. Growth, nodulation and yield responses of soybean (Glycine max L.) cultivars to rhizobia inoculation in two agroecological zones of Cameroon. Agronomy 9 (9), 540. https://doi.org/10.3390/agronomy9090540.

Nocedal, J., Wright, S.J., 2006. Numerical Optimization (2nd ed.). Springer.

Özkan, B., Dengiz, O., Turan, İ.D., 2020. Site suitability analysis for potential agricultural land with spatial fuzzy multi-criteria decision analysis in regional scale under semi-arid terrestrial ecosystem. Scientific Reports 10 (1), 22159. https://doi.org/10.1038/s41598-020-79105-4.

Pontius, R.G., Millones, M., 2011. Death to Kappa: birth of quantity disagreement and allocation disagreement for accuracy assessment. International Journal of Remote Sensing 32 (15), 4407-4429. https://doi.org/10.1080/01431161.2011.552923.

Saaty, T.L., 1980. The Analytic Hierarchy Process. McGraw-Hill.

Salvagiotti, F., Cassman, K.G., Specht, J.E., Walters, D.T., Weiss, A., Dobermann, A., 2008. Nitrogen uptake, fixation and response to fertilizer N in soybeans: A review. Field Crops Research 108 (1), 1-13. https://doi.org/10.1016/j.fcr.2008.03.001.

Sengupta, S., Mohinuddin, S., Arif, M., Das, S., 2022. Assessment of agricultural land suitability using GIS and fuzzy analytical hierarchy process approach in Ranchi District, India. Geocarto International 37 (20), 6081-6101. https://doi.org/10.1080/10106049.2022.2076925.

Singh, R., Singh, H., Raghubanshi, A.S., 2021. Challenges and opportunities for agricultural sustainability in changing climate scenarios: A review on soil and water management strategies. Journal of Cleaner Production 309, 127351. https://doi.org/10.1016/j.jclepro.2021.127351.

Sumner, M.E., Miller, W.P., 1996. Cation exchange capacity and exchange coefficients. In Methods of Soil Analysis: Part 3 Chemical Methods (pp. 1201-1229). Soil Science Society of America.

VanderPlas, J., 2016. Python Data Science Handbook. O'Reilly Media.

Wilson, J.P., 2012. Digital terrain modeling. Geomorphology, 137 (1), 107-121. https://doi.org/10.1016/j.geomorph.2011.03.012.

Withanage, N.C., Wijesinghe, D.C., Mishra, P.K., Dissanayake, D.M.A.K., 2024. An ecotourism suitability index for a world heritage city using GIS-multi criteria decision analysis techniques. Heliyon 10 (12), e31197. https://doi.org/10.1016/j.heliyon.2024.e31197.

Zadeh, L.A., 1965. Fuzzy sets. Information and Control 8 (3), 338-353. https://doi.org/10.1016/S0019-9958(65)90241-X.

Zhang, J., Su, Y., Wu, J., Liang, H., 2015. GIS based land suitability assessment for tobacco production using AHP and fuzzy set in Shandong province of China. Computers and Electronics in Agriculture 114, 1-11. https://doi.org/10.1016/j.compag.2015.03.007.

Zhang, J., Wang, C., Yang, C., 2020. Assessing the efficiency of sustainable agriculture development in China. Sustainability 12 (12), 5154. https://doi.org/10.3390/su12125154.